Title

Earthquake soil-structure interaction of nuclear power plants, differences in response to 3-D, 3 × 1-D, and 1-D excitations

Journal

Earthquake Engineering and Structural Dynamics, 47(6)

ISSN

0098-8847

Authors

Abell, JA
Orbović, N
McCallen, DB
et al.

Publication Date

2018-05-01

DOI

10.1002/eqe.3026

Peer reviewed

Earthquake soil-structure interaction of nuclear power plants, differences in response to 3-D, 3 × 1-D, and 1-D excitations

José A. Abell[1] Nebojša Orbovic´[2] David B. McCallen[3] Boris Jeremic[3,4]

[1]Facultad de Ingeniería y Ciencias Aplicadas, Universidad de los Andes, Santiago, Chile [2]Canadian Nuclear Safety Commission, Ottawa, ON, Canada [3]Lawrence Berkeley National Lab, Berkeley, CA, USA [4]Department of Civil and Environmental Engineering, University of California, Davis, CA, USA

Correspondence José A. Abell, Facultad de Ingeniería y Ciencias Aplicadas, Universidad de los Andes, Mons. Álvaro del Portillo 12.455, Las Condes, Santiago 7620001, Chile. Email: jaabell@uandes.cl

Summary

In soil-structure interaction modeling of systems subjected to earthquake motions, it is classically assumed that the incoming wave field, produced by an earthquake, is unidimensional and vertically propagating. This work explores the validity of this assumption by performing earthquake soil-structure interaction modeling, including explicit modeling of sources, seismic wave propagation, site, and structure. The domain reduction method is used to couple seismic (near-field) simulations with local soil-structure interaction response. The response of a generic nuclear power plant model computed using full earthquake soil-structure interaction simulations is compared with the current state-of-the-art method of deconvolving in depth the (simulated) free-field motions, recorded at the site of interest, and assuming that the earthquake wave field is spatially unidimensional. Results show that the 1-D wave-field assumption does not hold in general. It is shown that the way in which full 3-D analysis results differ from those which assume a 1-D wave field is dependent on fault-to-site geometry and motion frequency content. It is argued that this is especially important for certain classes of soil-structure systems of which nuclear power plants subjected to near-field earthquakes are an example.

KEYWORDS: domain reduction method, soil-structure interaction, wave propagation

1 INTRODUCTION

In soil-structure interaction (SSI) modeling of systems subjected to earthquake motions, it is usually assumed, often implicitly by just using a particular software, that the incoming earthquake wave field is a unidimensional, vertically propagating plane wave. Its been recommended for 40 years now “that soil-structure interaction studies should not be limited to seismic excitations with vertical incidence.”[1] Still, recent guidelines like the (2012) National Earthquake Hazards Reduction Program (NEHRP) SSI for Building Structures recommendations[2] implicitly assume a vertically incident plane-wave input motion for virtually all modeling recommendations and example applications. The plane seismic wave–field assumption is useful

because it tremendously simplifies the boundary conditions of the problem and because it enables the direct use of recorded motions in seismic response analysis. On the other hand, it introduces a modeling idealization, the implications of which are still poorly understood and an topic of active research.

The 1-D seismic wave–field assumption implies that horizontal components of surface motion can only be produced by vertically propagating horizontally polarized shear waves while the vertical component is produced exclusively by vertically propagating laterally constrained compressional waves. But it is known that the vertical component of surface motions is produced by a combination of inclined compressional and shear waves as well as surface waves. This complexity in the earthquake wave field and its potential to significantly affect the response of structures subjected to it was recognized by Housner[3] as early as 1956. He argued that what we now call wave-passage effects could reduce demands on structures with large in-plan extents and rigid foundations. The approach to simplifying these motions to a single input motion is known as the “base averaging.”[4] This view was later revised by Trifunac et al[5, 6] who advanced the idea that the effect, while real to some extent, is exaggerated by assuming a perfectly rigid foundation.[7] Reality shows that foundations do deform during motion, suppressing part of this effect.[8, 9] Additionally, wave-passage effects due to a nonvertically incident plane wave field have been linked to amplified rocking as well as torsional response of structures.[7, 10-14] Furthermore, it has also been claimed that under certain circumstances, wave passage can amplify structural response with respect to the vertically incident case[15] for long structures. These extremes, response reduction in one case and amplification in another, hint that the problem of seismic SSI is probably best studied case by case: a specific structure on a specific site experiencing an earthquake from a specific source.

Early on, response of structures to an obliquely incident plane body wave field or surface wave fields including SSI was addressed using analytical methods.[1, 11, 16, 17] With these methods, a working understanding of the possible effects of wave-field obliquity was established. It was recognized that buildings with large in-plan extents are sensitive to wave-passage effects and can experience enhanced rocking and torsional response. Moreover, high-frequency components of structural response display a greater sensitivity to the 3-dimensional characteristics of wave propagation than low frequency ones. Greater insight has been gathered on the subject recently by Trifunac et al,[7, 13] where a detailed 2-D nonlinear numerical model subject to different phases of plane waves was used to establish the importance of wave incidence angle and phase type in the response of buildings. Such studies further point towards the inadequacy of assuming vertical propagation as input motions.

In the light of this, it is apparent that nuclear power plants (NPPs) have characteristics that make them especially sensitive to the 3-dimensional

character of seismic wave fields. First, they are stiff structures usually with short fundamental periods. Second, NPPs have large lengths in plan and are usually founded on stiff soils of high strength, implying that several wavelengths of seismic motion will “fit” within the area of the NPPs at frequencies of input of engineering interest. Therefore, NPPs can transmit high-frequency motions to its components and equipment very efficiently. Third, the contents of NPPs are sensitive to accelerations (such as piping, heavy equipment, and their connections) and to displacements such as fluid sloshing and differential movement of interconnected components.

Near-field earthquake events, that is, events that occur near an NPP site (typical distance from site to source less than 20 km), pose a special kind of threat to NPPs. Despite the fact that NPPs would not likely be emplaced near a potentially active fault, NPPs have been built unknowingly near active faults that have been discovered after construction is completed.[18, 19] Data for events generated at these nearby faults are usually scarce to nonexistent, such that the only feasible way to obtain detailed, 3-dimensional ground motions is through numerical simulation. For nearby events, the wave-front in the near-field shows the curvature of initial propagation, such that a plane-wave approximation of this surface might not be satisfactory. Additionally, the high-frequency components of motion are less damped because there has not been enough propagation distance to produce significant attenuation. Therefore, small magnitude nearby events can produce high demands on a structure and its contents for some performance metrics, which are hard to anticipate, and there are reasons to suspect that plane-wave approximations of seismic field—even inclined ones—are not suitable. Advantageously, modeling and simulating near-field events is less computationally expensive than far-field events due to the reduced domain size that needs to be included in the wave propagation computation. Propagation domain sizes of a few to tens of kilometers, resolving frequencies of engineering interest, are well within the capacity of modern small-scale high performance computing (HPC) clusters or cloud-based resources.

Therefore, in the present work, the adequacy of vertically incident plane-wave approximations to seismic wave fields from near-field sources is evaluated in terms of the differences in response produced on a model of a generic NPP. This is accomplished by using seismic simulations of motions set off by a near-field source, and coupling them with a local site and structure finite element model through the domain reduction method (DRM).

The DRM, derived in the pioneering work of Bielak et al[20] and numerically demonstrated by Yoshimura et al,[21] allows coupling of realistic seismic waveform simulations with time-history analysis of a soil-structure system in such a way that the full 3-dimensional character of seismic waves can be propagated into a finite element model without further assumptions. Its usage requires detailed knowledge of the incident seismic wave field on all points located along a boundary of finite elements that encompasses the

soil-structure system with an adequate spatial resolution (less than 1 m for high-frequency applications). Such a dense characterization of the incoming wave field at the boundary nodes can only be obtained, as was envisioned by Bielak et al, by simulation of the propagation phenomenon from source to site. This can come at high computational cost.

To get around this, approaches to using DRM for SSI simulations in the past have simplified the problem to a 1-D wave field matching a seismic record. Refer, for example, to Psarropolous et al,[22] Jeremić et al, [23, 26] Kontoe et al,[24] Tripe et al,[25] Zhong and Huang,[27]and Solberg et al.[28] Alternatively, some studies do compute fully 3-dimensional DRM motions from a wave-propagation direct simulation approach but with a limited bandwidth, for example, Bielak et al[20] and Yoshimura et al.[21] With recent advancements in HPC, the ability to exploit the full potential of the DRM is continuously increasing as a result of the capability for executing ever larger, higher resolution regional scale ground motion simulations that can model extended faults and resolve frequencies of engineering interest. The work of Isbiliroglu et al[29] is a good example of the usage of DRM in conjunction with a 3-D extended fault model, in a spatially heterogeneous medium, applied to the quantification of the effects of clusters of simplified buildings on ground motion, as well as those of SSI in individual structures and of structure SSI between buildings, for frequencies up to 5 Hz.

A more “classical” approach to seismic SSI involves inputing the (1-D) wave field as a stress input at a given depth under the model and capturing out-going motions with Lysmer-type boundaries.[30, 31] Examples of this approach include Elgamal et al,[32] Ostadan et al,[33] and Coleman et al[34] to name a few.

In this scenario, physical modeling of the complete earthquake soil-structure interaction (ESSI) problem is possible using DRM to couple a detailed local model of site and structure with high performance, validated models of earthquake sources and regional wave propagation properties. This is both practical and necessary to show adequate seismic response of structure, especially NPPs, to these events.

The main idea in this article is to determine, using DRM, if the response of a structure excited by a plane and vertically propagating input wave field is different from the one excited by the full 3-D wave field, even when these fields are identical at the point of emplacement of the structure. For this purpose, it will suffice to use a linear model of the NPP and site as well as simple point source for the earthquake because the differences—it is postulated—will arise even in this simplified setup as a basic feature of the physical phenomenon at hand.

A simplified NPP model was created in the real ESSI simulator system[35] developed at the University of California at Davis and Lawrence Berkeley National Lab. Earthquake motions were input into the SSI system using equivalent forces obtained via the DRM. These forces were obtained by evaluating the response of the seismic wave propagation problem at the

nodes located at the DRM boundary, for any given source. Earthquakes were modeled as dip-slip point sources, at varying depths and with an adequate frequency content. For the motions produced at each source depth, 3 types of DRM input motions were developed: “Full 3-D” motions, which correspond to the direct input of the motions produced by the seismic simulations into the model; “1-D” motions, which are a 1-component, vertically propagating plane-wave approximation to the full 3-D motions; and “3 × 1-D” motions, which are a 3-component vertically propagating plane-wave approximation to the full 3-D motions. Both plane-wave approximations were obtained by performing 1-D motion deconvolutions of the recorded motion at the NPP site.

From the simulated 3-D seismic wave field, ie, the “free-field” surface motions computed at the NPP site using the seismic simulation, vertically incident plane wave–field approximations are developed by deconvolving each component of motion independently. Deconvolutions are conducted in the SHAKE91 program[36] for 1-D site response analysis (see considerations by Mejía and Dawson[37]). For horizontal components, a vertically incident, horizontally polarized pure shear wave field is assumed, using shear-wave speed and density assumed for the site. For the vertical component, a laterally constrained vertically propagating compression wave is assumed, hence the constrained modulus of elasticity and other properties. When only the horizontal component is used (as in many analysis cases), the resulting wave field is called, herein, a “1-D” wave. When all 3 components are deconvolved and input simultaneously, the resulting wave field is called “3×1-D” wave since 3 components are used, but they only depend on the depth and time. Finally, using the complete seismic wave is termed “full 3-D” wave field.

This approach differs from traditional approaches to SSI analysis in several ways. First, motions come from fully 3-dimensional source are propagated and coupled perfectly into the local FEM model using DRM. This means that no-plane wave assumption is made and all wave phases are inherently considered. Second, frequencies up to 10 Hz are resolved, which, while possibly insufficient to completely characterize NPP hazard, can be accomplished with modest computational resources and is enough to prove the point of the article. Last, the goal is to compare locally equivalent vertically incident plane-wave approximations of wave field, a state of practice, with the full 3-D approach to establish the consequences of such assumptions. The combination of all these modeling features serving this goal is the main novelty of this article.

The rest of the article develops as follows. Section 2 elaborates on the methods used to generate the full 3-D wave field from point source earthquake excitations and following through the propagation of the site, as well as the details regarding the deconvolution process used to develop 1-D and 3 × 1-D motions. Section 3 explains the “local” model used to represent the generic NPP and the local site used herein. Section 4 presents the results

obtained in terms of NPP response at different points. The response from a 3-D wave field is compared with 1-D wave field and is followed by comparing full 3-D with 3 × 1-D. Section 5presents the main analysis and discussion of the results in terms of the different modeling assumptions. Finally, Section 6 presents the main conclusions of this work.

2 GENERATING DRM MOTIONS

In this study, earthquake motions are generated using a fourth-order finite-difference code SW4, which solves for the fully 3-D elastodynamics equations.[38] The domain considered is a 10 km × 5 km × 5 km box, with the NPP site located at the middle of its top surface. Figure 1(left) shows this general setup.

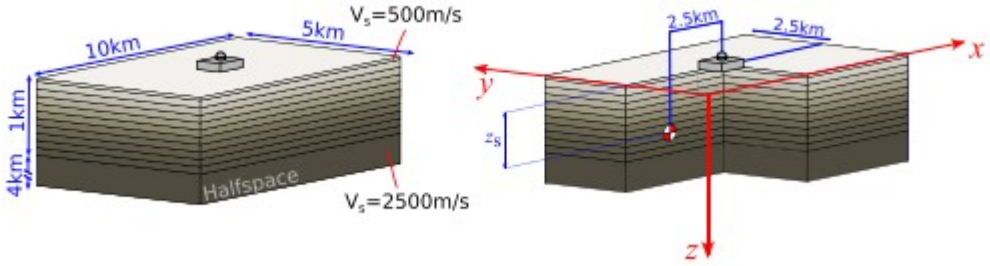

Figure 1

Geometry of local crust at nuclear power plant (NPP) site (left) and location of source earthquake relative to NPP site (right).

A horizontally layered elastic half-space is used to model the crust in the region around the NPP site. In full 3-D modeling with finite-differences, the model must contain both the source and the site. Ten homogeneous layers with shear-wave speeds from V_s=500 m/s at the top to V_s=2500 m/s at the bottom of the model represent the variation of crustal properties within the first 1 km of depth. Properties at greater depths are assumed constant. Table 1 reports these and other properties used in all layers of regional model. The chosen setup is meant to represent a generic site for a nuclear power facility, which usually feature rock or high-strength soils.

TABLE 1 Properties of the layers used in the regional model

V_p, m/s	V_s, m/s	ρ, m/s	z_1, m	z_2, m
1000	500	2000	0	50
1894	947	2018	50	100
2265	1132	2035	100	200
2789	1394	2070	200	300
3191	1595	2105	300	400
3530	1765	2140	400	500
3828	1914	2175	500	600
4098	2049	2210	600	700
4347	2173	2245	700	800
4578	2289	2280	800	900
4795	2397	2315	900	1000
5000	2500	2350	1000	∞

Note. V_p, speed of primary waves; V_s, speed of secondary waves; ρ, density; z_1, depth of the top of the layer; z_2, depth of the bottom of the layer.

Reverse faulting earthquakes, modeled using point-source double-couple mechanisms, are placed at a distance of 2.5 km away from the NPP site in the x direction at source depths (z_S) of 550, 850, and 1200 m. This is depicted in Figure 1 (right). Large events might be modeled as a superposition of these types of sources with properly scaled magnitudes and delays given by the rupture propagation front. At least for a linear analysis, differences arising from comparing full 3-D wave field with equivalent 1-D or 3 × 1-D ones would arise in even the case of having a point-source.

Capturing an adequate frequency content for the resulting motions is very important for a realistic analysis using point sources. Brune[39, 40] derived the shape of the source-time function based on physical considerations of the available stress to drive the near-fault acceleration of a rupturing fault. A smoothed version of the Brune source-time function, with a corner frequency of f_0=10 Hz, was used herein. The seimic source model therefore consists of single double-couple point sources at 3 source depths (z_s={550 m,850 m,1200 m}). Faulting mechanism assumes a reverse-fault at 45° dipping angle towards the direction of the NPP. The simulated displacement response of the elastic medium is recorded at the site of the geometric center of NPP foundation, which is then used to produce equivalent 1-D and 3 × 1-D wave fields for comparison. Motions are also recorded at the locations of the FEM mesh nodes on the DRM boundary and used to develop DRM forces. Because the seismic model grid points and FEM mesh nodal points do not exactly match in space as a result of different discretization sizes, a nearest-neighbor approach is used to assign motions from the seismic simulation into each DRM node. Free-field studies using the FEM to predict site motions from the DRM input, reported elsewhere,[41] show good agreement between target motions at the site computed with DRM. All seismic simulations were conducted using the finite-difference code SW4, on the Lawrence Berkeley National Laboratory National Energy Research

Scientific Computing Center's (NERSC) “Edison” supercomputer using 512 processors running for about 5 hours.

To remove the effect of geometric attenuation and focus the work on the source-to-site geometry effect, all motions were scaled to obtain a 1 cm maximum displacement in the horizontal component, other components being scaled accordingly. This allows a fair comparison of the relative importance of the presence of 3-D effects (such as surface waves), at least in the linear analysis case, for a given stress drop. The scaling and overall treatment of the fault rupture specification are not meant to be representative of a specific real rupture, rather its meant to emphasize the point that differences between a fully 3-D analysis and equivalent 1-D or 3×1-D analyses arise from the 3-D nature of problem even in the most basic circumstances.

Figure 2 shows the displacement and accelerations recorded at the NPP site for the different source depths after scaling. Motions occurring at frequencies above , unresolved frequencies, appear as high-frequency noise and were filtered out by a forward-backward fourth-order Butterworth filter before application to the local model. Note the enhanced presence of surface waves for the shallow-source cases, which manifests as a delayed wave (after t=2.0 s).

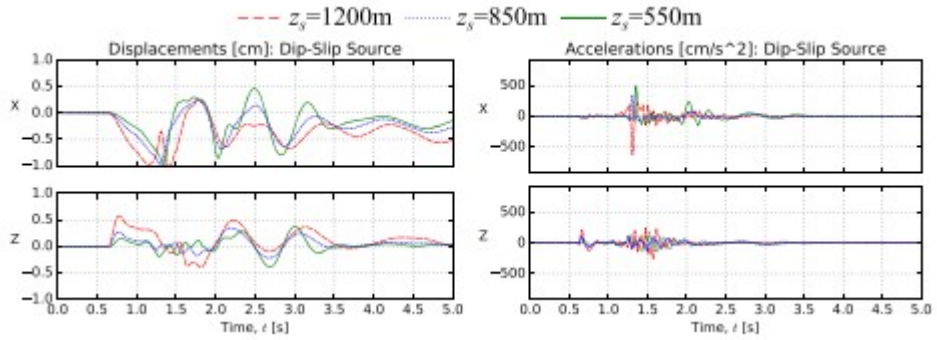

Figure 2

Synthetic records produced by point sources at varying depths, recorded at the site of the nuclear power plant. Records are scaled to have 1 cm of maximum horizontal displacement

Figure 3 shows the absolute value of the discrete Fourier transforms for the same records shown in Figure 2. Note the high-frequency decay rate of the spectrum, starting at the corner frequency, of 2 orders of magnitude per decade ω^{-2}, characteristic of the Brune source-time function.

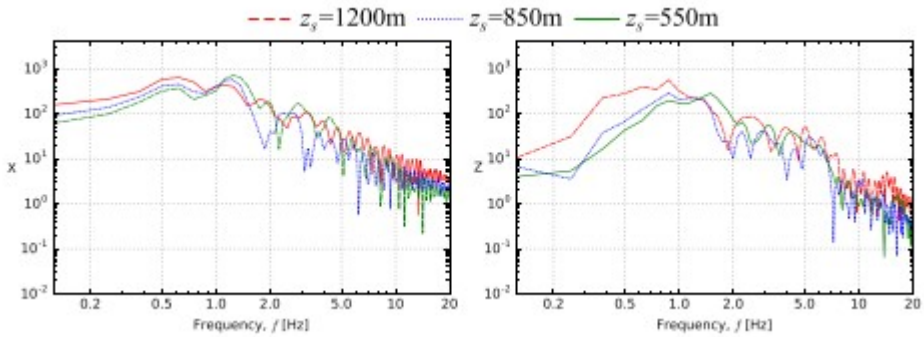

Figure 3

Discrete Fourier transforms of the (unfiltered) displacement records shown in Figure 2

From the simulated 3-D seismic wave field, ie, the “free-field” surface motions computed at the NPP site using the seismic simulation, vertically incident plane wave–field approximations are developed by deconvolving each component of motion independently. Deconvolutions are conducted with a customized version of the SHAKE91 program[36] for 1-D site response analysis (see considerations by Mejía and Dawson[37]). SHAKE91 is a 1-D equivalent linear site response analysis program, as such it only requires a single wave speed (or modulus) and density to specify propagation properties. For horizontal components, the SHAKE91 output is interpreted as a vertically incident horizontally polarized pure shear wave field; therefore, the shear-wave speed and density at the site are used. For the vertical component, SHAKE91 output is interpreted as a laterally constrained vertically propagating compression waves, which requires that the speed of constrained compression waves and density be used as main parameters. When only the horizontal component is used, the resulting wave field is called, herein, a “1-D” wave. When all 3 components of deconvolved motion are input simultaneously, the resulting wave field is called “3 × 1-D” wave since 3 components are used, but they only depend on the depth and time. Finally, using the complete seismic wave is termed “full 3-D” wave field.

Because the ground motions were generated using a smooth source-time function, a simple layered crust with heterogeneous isotropic elastic material and no damping, and because care was taken to filter out unresolved frequencies, the ground motions at the surface will be highly coherent when time-lag is removed. This is important in the interpretation of the results, where the only source of difference is the 3-D character of the “full 3-D” wave field compared to the plane-wave approximation of this motion.

3 NPP MODELING

Figure 4 shows a drawing of a generic NPP used as an example structure in this work. Shown are plan and elevation views featuring both the containment as well as the auxiliary building. The structure has a 1:1 in-plan aspect ratio. Posttensioned and reinforced concrete walls with thicknesses ranging from 0.4 m to 1.6 m are spaced every 12.5 m within the auxiliary

building. The containment building consists of a 40-m-diameter and 40-m-high cylinder capped by a dome, with 1.6 m of wall thickness. The NPP has a 3.5-m-thick continuous foundation slab.

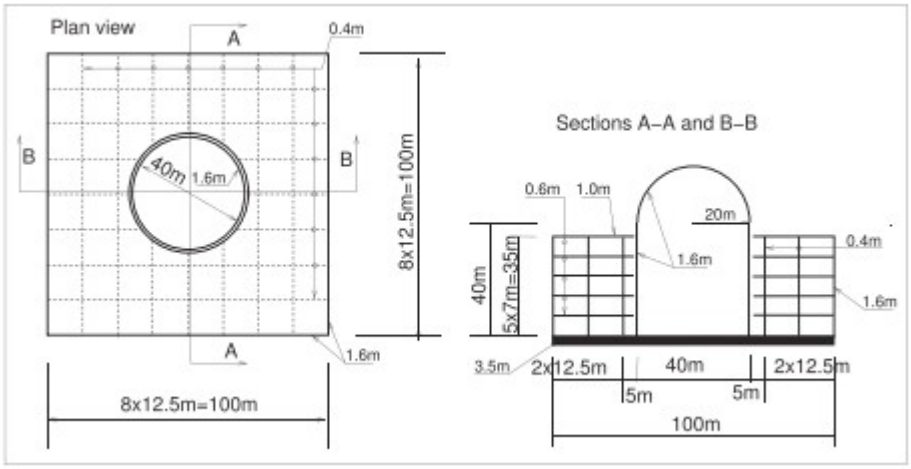

Figure 4

Nuclear power plant geometry

The gmsh[42] meshing program was used to construct a 3-dimensional geometrical model of the NPP and produce a mesh composed of hexahedral finite elements for soil and foundation slab and quadrilateral shell elements for the walls and slabs of the auxiliary building as well as the containment building.

Figure 5 shows an overall and an internal view of the generated mesh. The model uses shell elements for containment and auxiliary building and brick elements for foundation slab and soil. The soil volume is separated in an internal domain, a DRM boundary (1 layer), and an absorption layer of elements outside of the DRM boundary, which is used to damp any out-going wave motion. The absolution layer is important, because it captures the waves radiated outward from the domain due to the motion of the NPP. These waves are not canceled by DRM because the input motions used to derive DRM forces only include free-field motions. The DRM layer is placed at a distance of 40 m away from the NPP edges. Therefore, the internal soil box has dimensions 180×180×40 m.

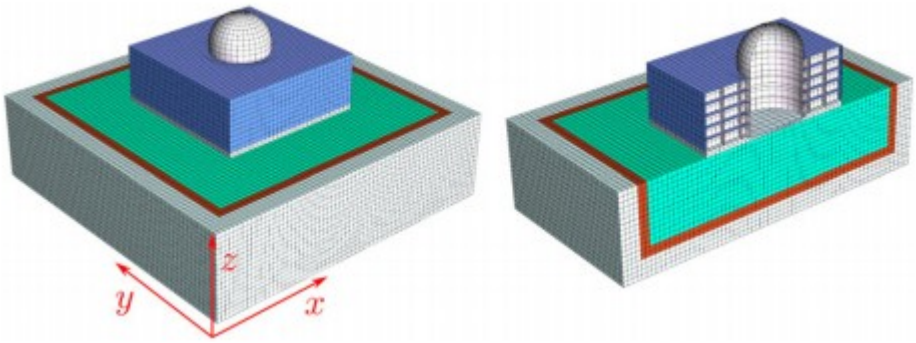

Figure 5

FEM mesh of the site and nuclear power plant featuring, in orange, the layer of domain reduction method elements

The discretization of the model is controlled by the discretization of the free-field, which is controlled, in turn, by the desired accuracy of wave propagation. Accurately resolving the wave amplitudes for a given maximum frequency imposes restrictions on the spatio-temporal discretization, which are more stringent than just meeting the Nyquist criterion.[43]For finite elements with linear displacement interpolation functions involving linear material and geometrical response, it has been shown many times (see Watanabe et al[44] for a recent discussion) that at least 10 elements per shortest wavelength are required to accurately resolve displacement amplitudes. In addition to that, the time step is limited by the Courant-Friedrichs-Lewy condition[45]; eg, the time step must be chosen such that the distance traveled by the fastest phase is less than the smallest spacing between grid nodes for all points in the mesh. In the present case, considering a target maximum resolvable frequency of 10 Hz and the selected surface shear wave velocity, a discretization of size dx=5 m is needed. Considering the aspects presented in the previous chapter and other geometrical constraints of the mesh, a mesh size of dx=3.2 m is selected for the soil. Within the DRM model, which has a uniformly spaced mesh, the fastest phase is the P-wave with V_p=1000m/s; therefore, the time step is chosen to meet dt<dx/V_p=3.2m/1000m/s=0.0032s. In practice, the time step of the SW4 output (0.00083s) is used.

The resulting mesh consists of 106 165 nodes, of which 9728 define 6 degrees of freedom (3 translations and 3 rotations) and 96 437 define 3 degrees of freedom. A total of 100 736 elements are defined, consisting of 31 824 shells and (68 912) 8-node bricks. A total of 37 632 of the continuum elements will contain material representing the soil, while the rest use materials representing the DRM layer, absorption layer, and foundation slab.

It is important to mention that, in the finite element model, all shear walls are extended into the foundation slab by adding additional embedded elements within it. This is important for the correct determination of out-of-

plane stiffness of the wall/foundation system, which would, otherwise, present an unrealistic hinged condition at the base in that direction.

The high-performance linear quadrilateral ANDES shell finite element formulation[46-49] implemented in Real ESSI is used herein. This element formulation is able to capture the vibrational dynamics of shells with high accuracy at the cost of forfeiting the concept of displacement interpolation functions. Given the thickness in shear walls for the auxiliary and containment buildings, and because these are often built using posttensioned concrete, a linear model for concrete behavior suffices.

A Rayleigh damping model is used to assign viscous damping to all parts of the domain. The damping ratio is set at 20% of critical for elements located at the DRM absorption layer, which is meant to model the radiation damping of the soil-structure system. For the soil elements, the damping is set to 5% with the idea that the soil will dissipate some additional energy due to localized hysteretic behavior. Finally, all concrete elements were assumed to remain linear and show reduced damping (cracking of concrete is avoided in NPP design); therefore, a 2% critical damping ratio was used for structural components and foundations.

The only physical role attributed to damping in this work is to absorb the out-going waves from the portion of motions not canceled by the DRM layer. Damping elsewhere in the model plays a cosmetic role, because damping is expected to occur. Indeed, the assignment of different damping values to different parts of the domain results in a nonclassical damping matrix, which makes the assessment and tuning of a global effective damping for a model of this size a hard task. Furthermore, the use of a mass-proportional damping term in the Rayleigh model is only justifiable in the case of the DRM absorption layer (similar to Lysmer dashpots) and, possibly, within the soil were it to be below the phreatic level (as soils in NPP sites usually are). No claim is made herein that damping terms other than those associated with the DRM layer play a physical role.

For reference, Figure 6 shows the first 5 fixed-base eigenmodes and eigen frequencies for both the auxiliary building and the containment building. The first 2 translational eigenmodes of the auxiliary have a frequency of 9.6 Hz, while the same modes for the containment building are at 6.1 Hz. This result is within the expected range for both buildings. Of course, the dynamics of the response of the NPP is governed not by the fixed-base modes but by the natural frequencies of the NPP including foundation and site, which have lower frequencies than the fixed-based modes, as will be shown.

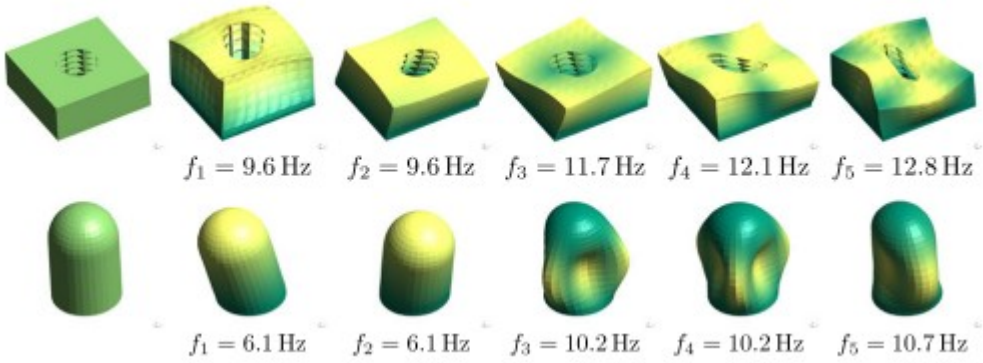

Figure 6

Undeformed shape and first 6 fixed-base eigenfrequencies and eigenmodes for auxiliary building (top row) and containment building (bottom row)

After postprocessing, the results from the SW4 simulations, nodal displacements were used to obtain nodal accelerations. Data and metadata necessary for DRM computations were stored in an HDF5 dataset designed for high-performance read operations for real ESSI. Simulations for the NPP and site were executed using DRM forces computed from these datasets. The simulations were run on 192 processors of the NERSC “Edison” cluster for approximately 4.5 hours.

4 RESULTS

Figure 7 shows the locations on the finite element model for the NPP where displacement responses were calculated, namely, at the bottom of foundation, top of containment building, and north-west corner of the auxiliary building. Figures 8 through 10 report results comparing full 3-D analysis with equivalent 1-D analysis, that is, considering only the horizontal component for the 1-D deconvolution of input motions produced by sources at the different depths considered. Next, Figures 11 through 13 report the response at the top of foundation and top of the containment building, this time comparing between full 3-D analysis and 3 × 1-D analysis, with input motions proceeding from the same source depths as before. For all cases, the displacement and acceleration time-history responses are shown.

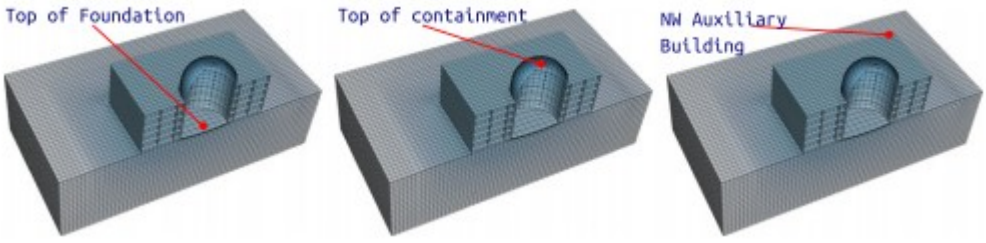

Figure 7

Positions on the nuclear power plant FEM model where the response is reported

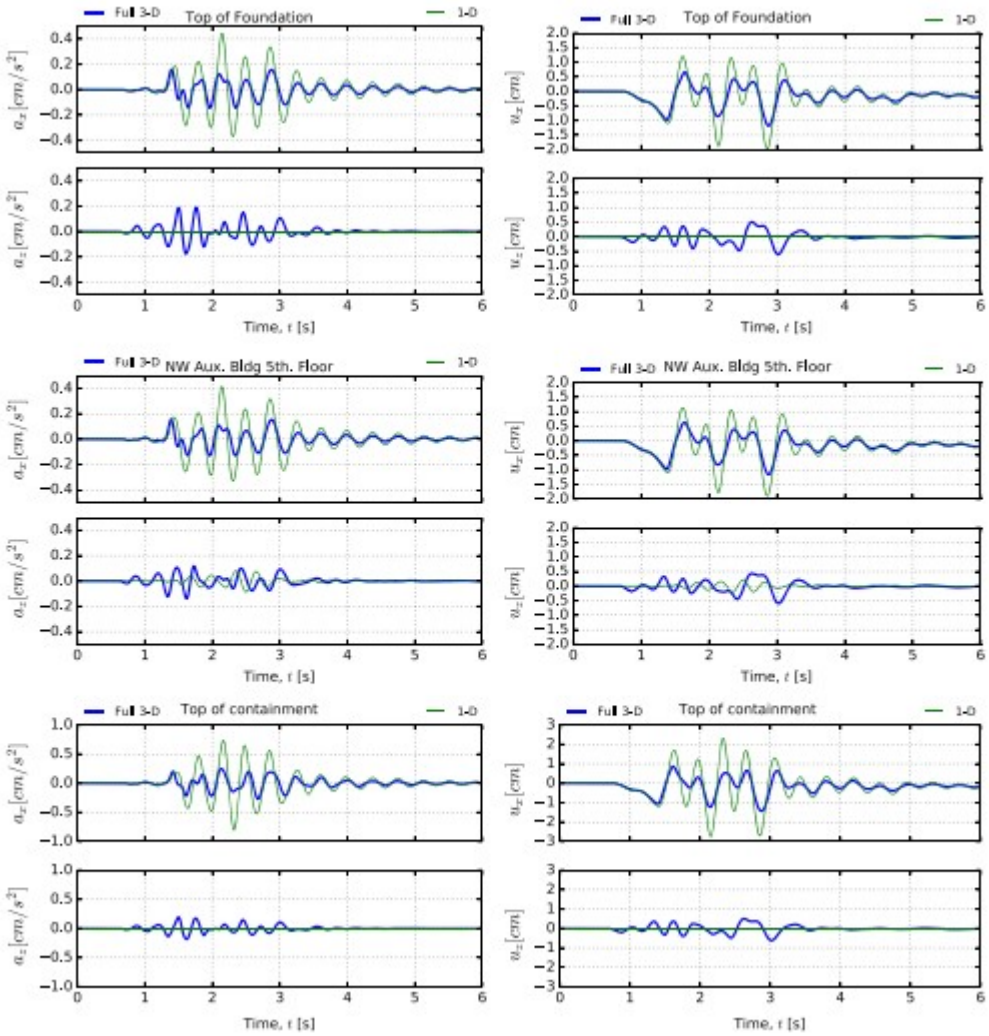

Figure 8

Response of the nuclear power plant to the motions produced by a source at z_s=550 m comparing full 3-D analysis with equivalent 1-D analysis

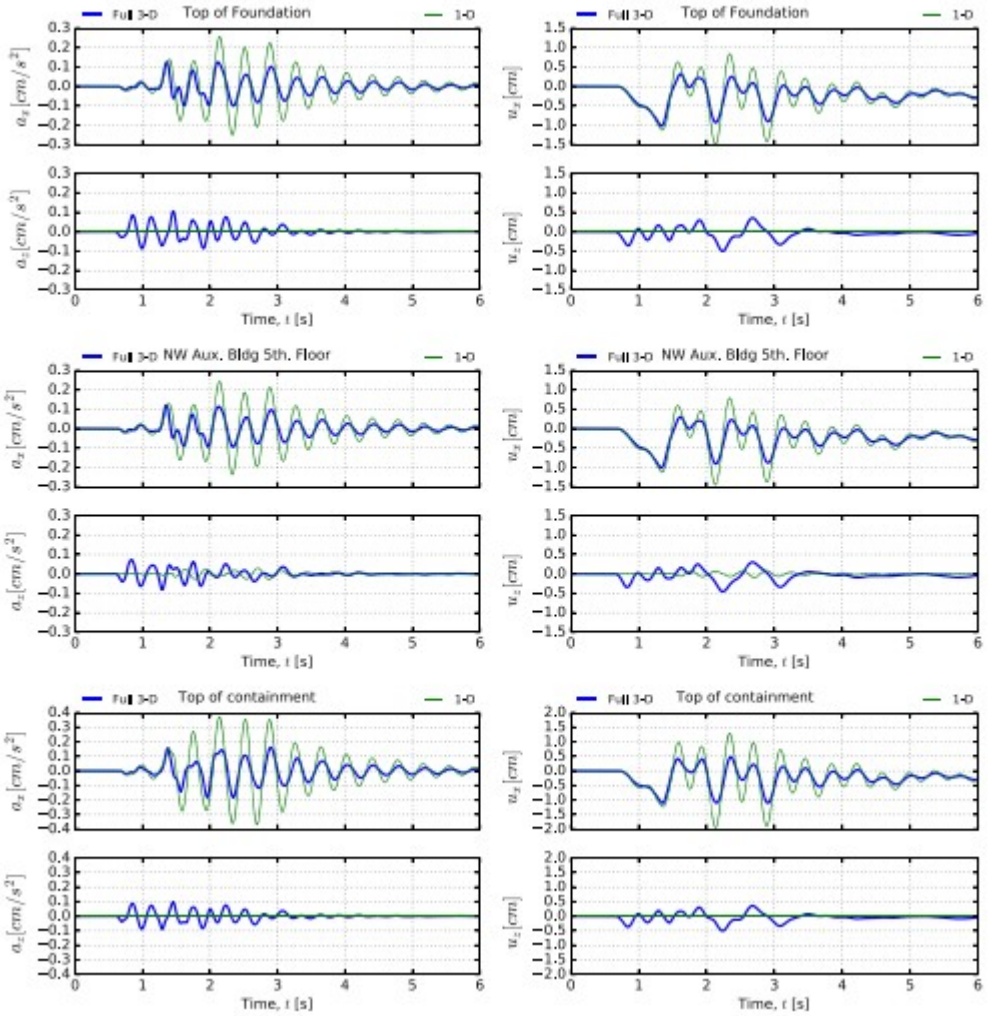

Figure 9

Response of the nuclear power plant to the motions produced by a source at z_s=850 m comparing full 3-D analysis with equivalent 1-D analysis

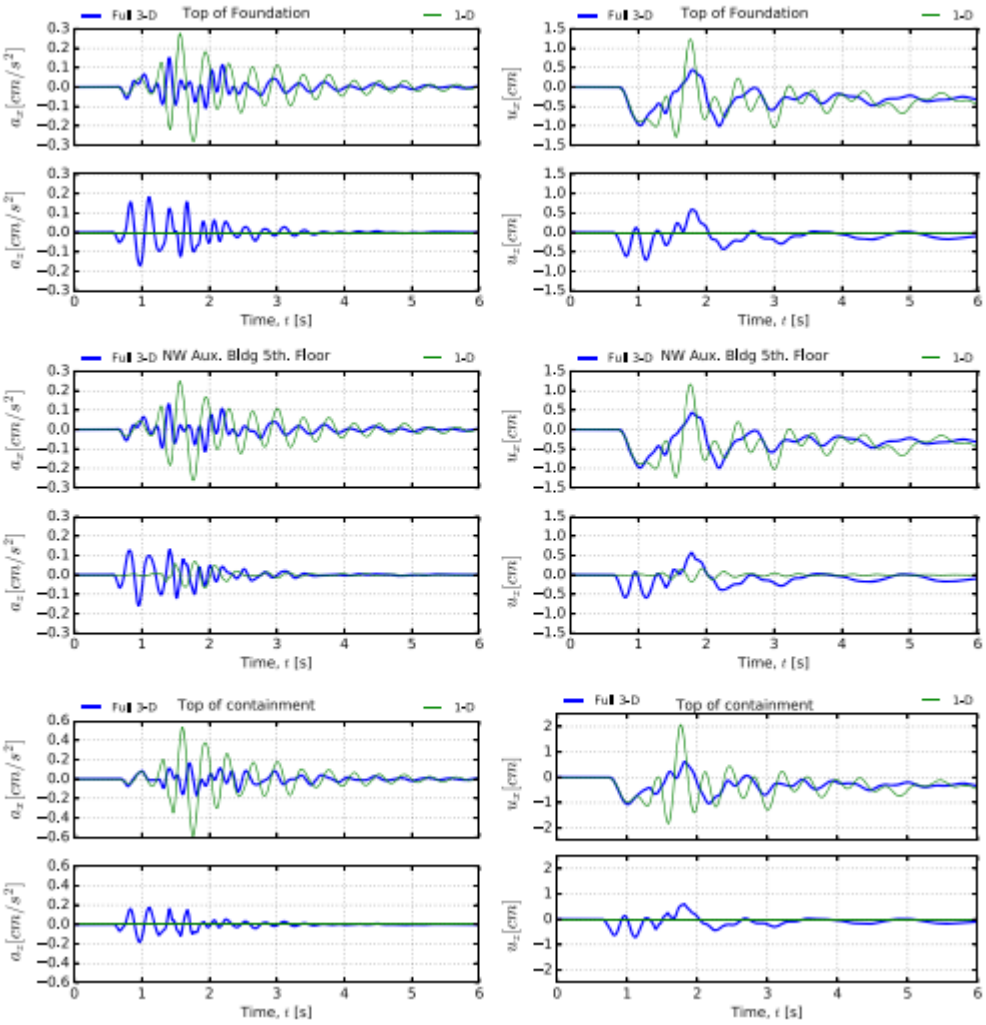

Figure 10

Response of the nuclear power plant to the motions produced by a source at z_s=1200 m comparing full 3-D analysis with equivalent 1-D analysis

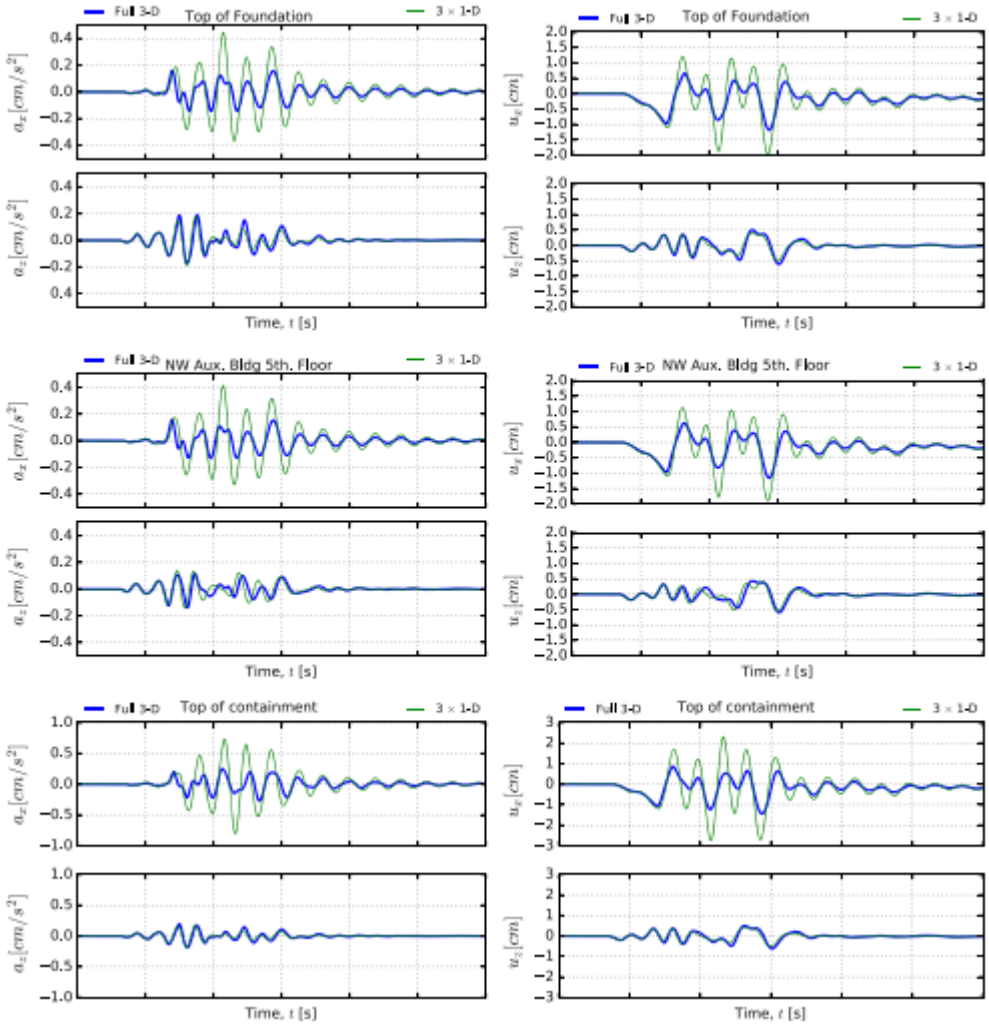

Figure 11

Response of the nuclear power plant to the motions produced by a source at z_s=550 comparing full 3-D analysis with equivalent 3 × 1-D analysis

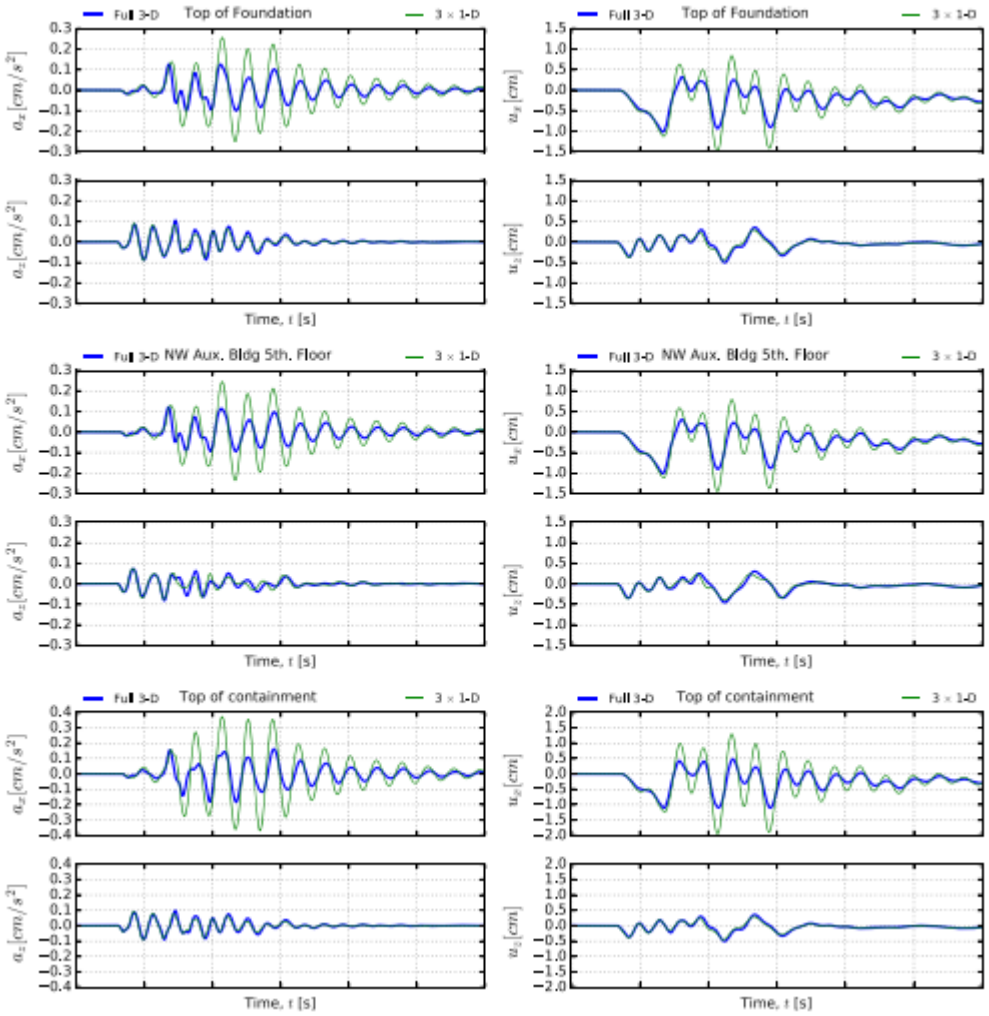

Figure 12

Response of the nuclear power plant to the motions produced by a source at z_s=850 comparing full 3-D analysis with equivalent 3 × 1-D analysis

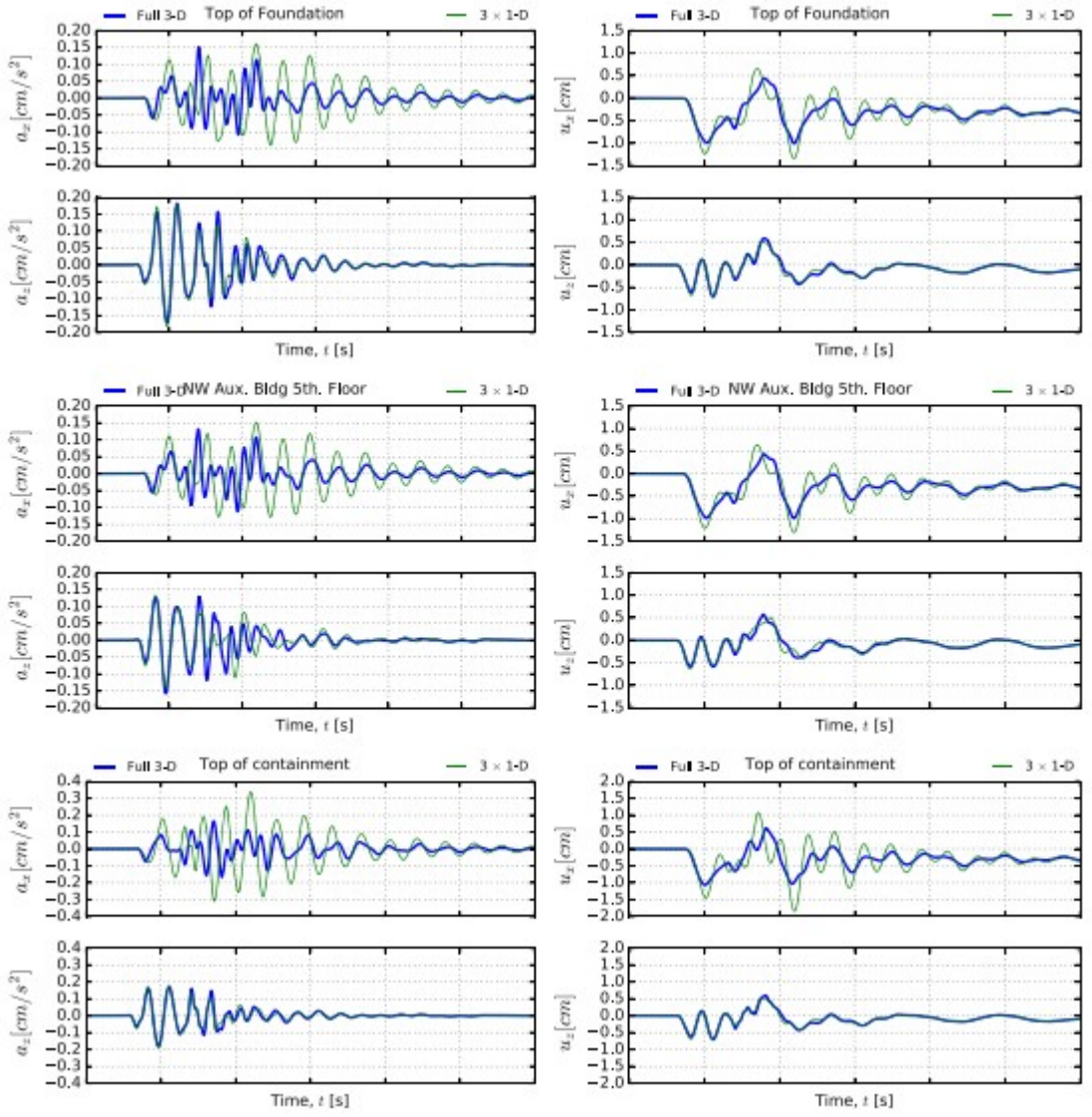

Figure 13

Response of the nuclear power plant to the motions produced by a source at z_s=1200 comparing full 3-D analysis with equivalent 3 × 1-D analysis

Figure 14 presents the comparison of the Fourier response spectra for the motions recorded at the top of the containment building for sources of varying depths, using full 3-D and 1-D analyses. Figure 15 presents the same plots, now comparing with 3 × 1-D analysis.

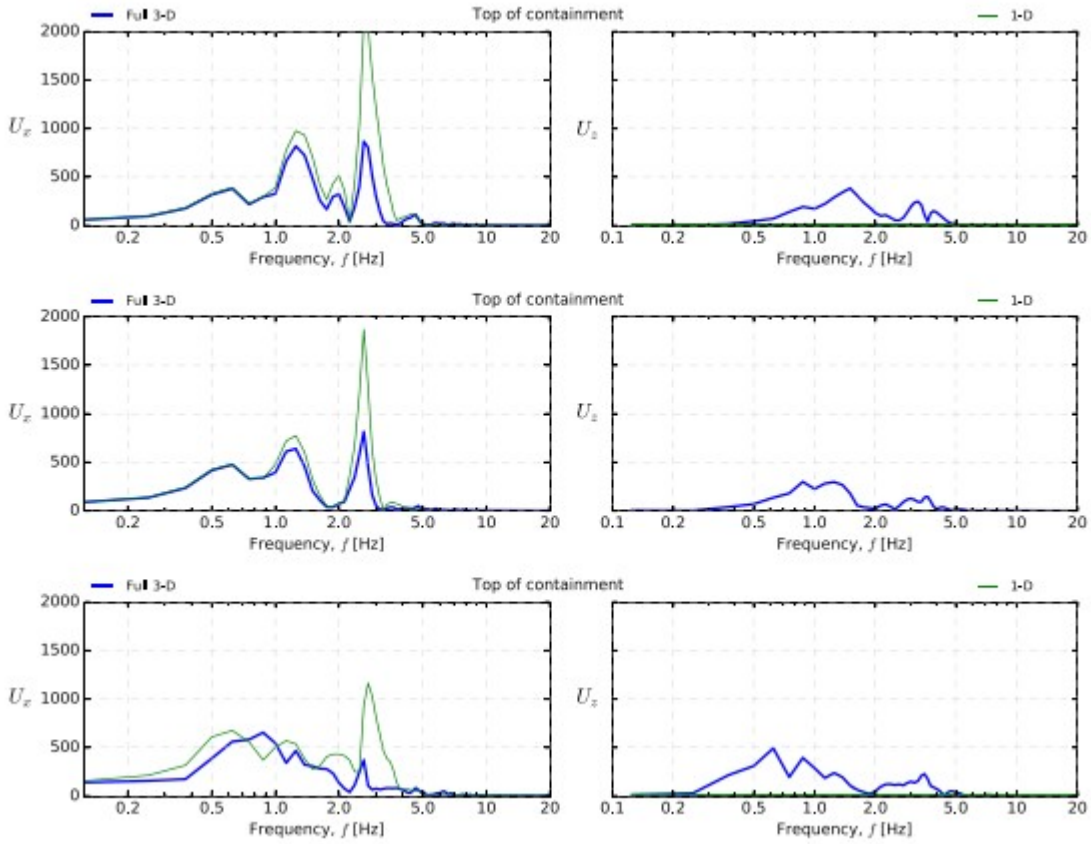

Figure 14

Fourier response of the nuclear power plant to the motions produced by a source at z_s=550 m (top), z_s=850 m (middle), z_s=1200 m (bottom) comparing full 3-D analysis with equivalent 1-D analysis

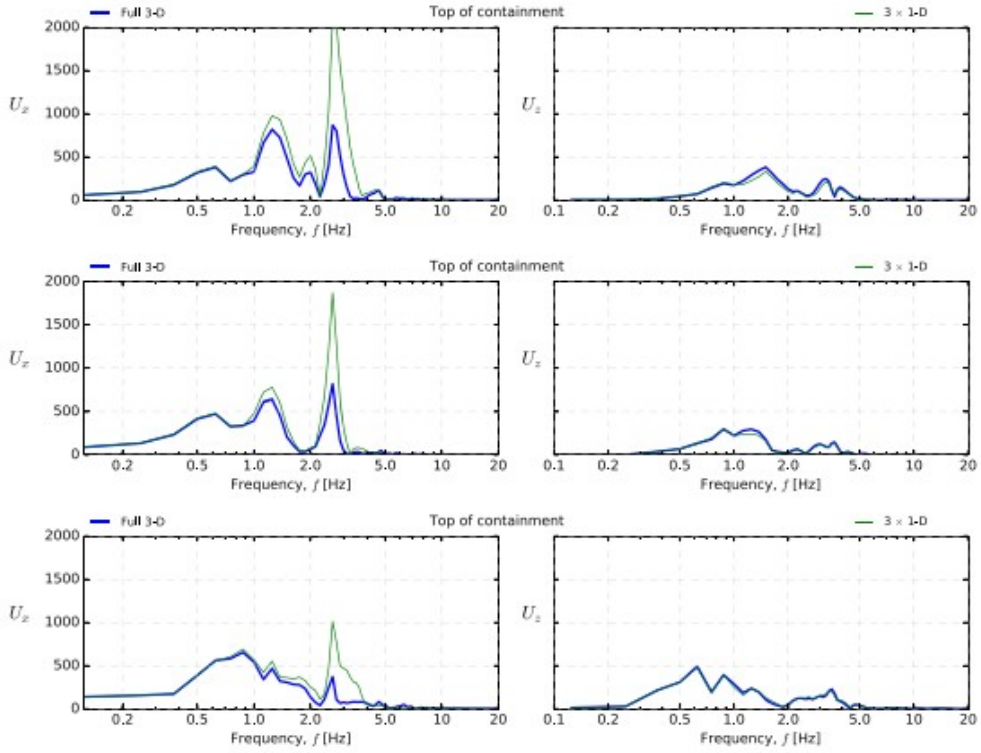

Figure 15

Fourier response of the nuclear power plant to the motions produced by a source at z_s=550 m (top), z_s=850 m (middle), z_s=1200 m (bottom) comparing full 3-D analysis with equivalent 3 × 1-D analysis.

Finally, Figure 16 shows deformed shapes of NPP and site at an instant in time due to a z_s=550 m fault using the different types of input motions, allowing to assess the overall differences in response throughout the building.

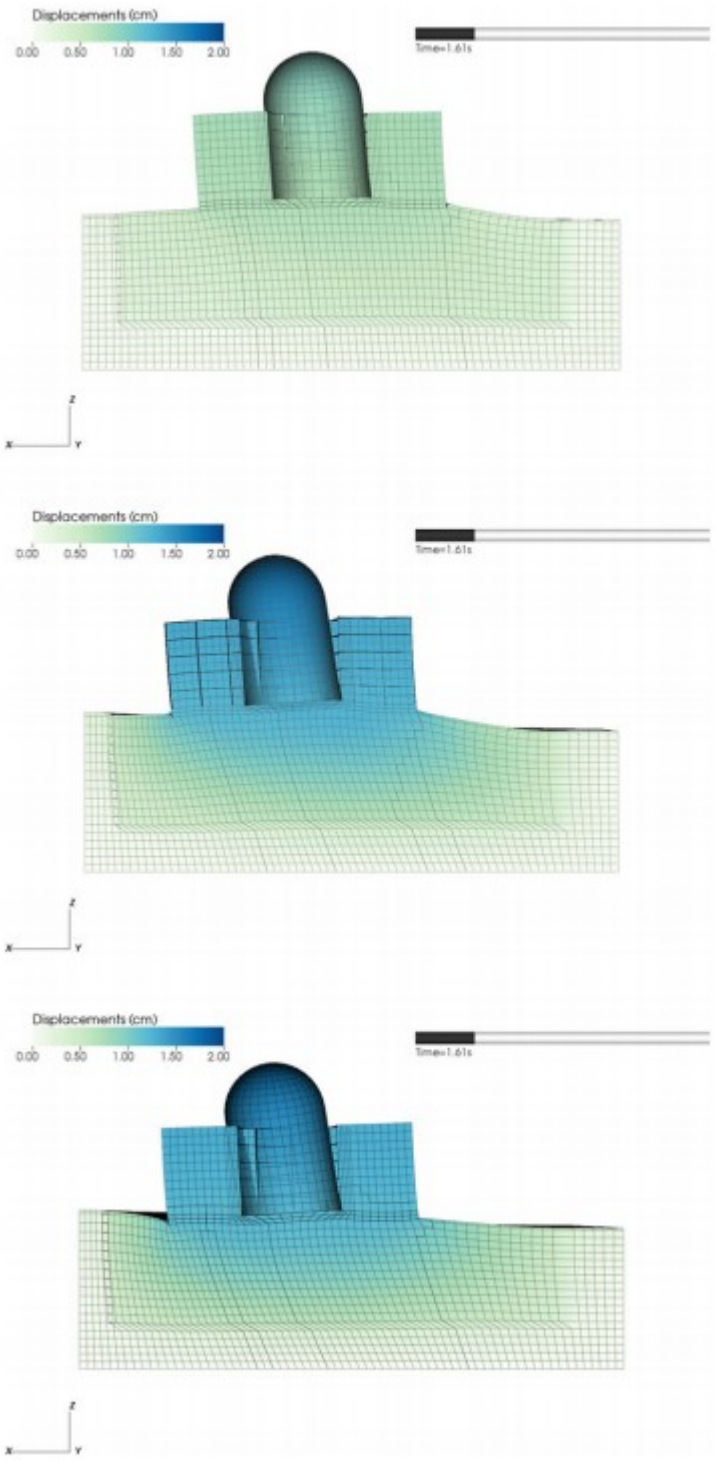

Figure 16

Deformed shape of the nuclear power plant and site (exaggerated) at time t=1.61 s for source at z_s=550 m. The top shows full 3-D analysis, while the middle and the bottom show equivalent 1-D and 3 × 1-D analyses. Note that the deformation at the far edges (free-field) are nearly identical

5 DISCUSSION

A simple calculation using Snell law, which relates the ratio of the wave speeds with the ratio of the sines of the incidence angles ( ), shows that for a 45° dipping fault, which is a source of S-waves inclined at 45°, the incidence angle measured from the vertical at the surface would be θ=10.6°, 8.9°, and 8.1° for the faults located at z_s=550, 850, and 1200 m, respectively. Therefore, the wave field has an approximately vertical angle of incidence at the site. Using a typical argument in SSI research and practice, even for this simplified numerical experiment, the wave field is an almost vertically propagating S-wave. This would be then used to argue in favor of using a 1-D or 3 × 1-D approach to modeling the seismic wave field. In this study, P-wave and S-wave speeds are in a 2:1 ratio, so incidence angles are affected in the same way for both phases. In general, different wave phases will reflect and diffract depending on their particular speed ratio.

From the results presented in the previous section, it can be readily inferred that the responses of the NPP to a full 3-D, 3 × 1-D, and 1-D wave field are different, even if the latter two were developed using a state-of-practice approach of deconvolving the motion in depth. Notably, the deconvolution method matches perfectly the recorded motion at the site of the NPP when only free-field motions are considered. This result reduces the credibility of the argument that a near-vertical incidence angle, computed via Snell law, suffices to establish the adequacy of a 1-D or 3 × 1-D SSI analysis for the purposes of establishing the earthquake-soil-structure response of structures.

Comparison with the results by Luco et al[17] in the case of close sources shows that wave-passage effects are more pronounced (ie, there seems to be more deamplification) than the ones obtained by those authors in the case of very near sources. Direct comparison, however, is not possible because of different layering structure and the consideration of a perfectly rigid superstructure in the case of Luco et al.

An overarching theme across all comparisons herein is that wave fields derived from deconvolution (1-D or 3 × 1-D) are associated with increased peak responses for both displacements and accelerations. This is because these wave fields deliver all the wave energy in phase, at the same time, across the span of the foundation. Conversely, in the full 3-D case, the motion starts at 1 foundation edge and traverses the whole foundation in a phased manner. This is due to the wave field being inclined as opposed to purely 1 dimension. In the unidimensional cases, the seismic motions propagate into the NPP structure and constructively interfere inside it. The delayed delivery of energy in the 3-D case means that the motions do not constructively (nor destructively) interfere inside the structure, resulting in reduced net response. This effect can be simplistically identified as the concept of kinematic interaction and is one of the rationale for the base-averaging effect (the other being motion incoherence). In this particular case, responses are reduced by about 50% from those computed with

deconvolved (1-D or 3 × 1-D) motions. The authors would like to stress that this is not a generalizable result.

Nevertheless, this aspect of response is very much a frequency-dependent one. Indeed, looking at discreet Fourier spectra across all examples (Figures 14 and 15), it is apparent that the 3-D, 1-D, and 3 × 1-D methods are coincident for low-frequency input except for the deep source where the 1-D method produces different results. Low frequencies are associated with long wavelengths. For example, for a frequency of 0.5 Hz, a corresponding S-wave will have around 1 km of length, which exceeds the size of the NPP foundation slab. Therefore, for these frequencies, the site motion approximates that of a rigid body, and it can be said that a 1-D wave field will be a good approximation. This is also in-line with the results reported in Luco and Sotiropoulos,[17] where it was noted that the wave-passage effect got worse with increasing frequency and decreasing distance to the fault.

At the high-frequency end of the Fourier response, it is seen that the 1-D and 3 × 1-D wave fields tend to deliver more energy, although not much can be said for frequencies higher that 5 Hz from these results.

Still with reference to Figures 14 and 15, notable peaks in the Fourier spectra occur at around 0.6 Hz, 1.3 Hz, and about 3 Hz. The first two are identified as source-related, because they can be identified in the free-field Fourier responses. The last peak is inferred to be the structure-site natural mode of vibration as measured at the top of the containment building, implying that the fundamental frequency of the containment building is halved when SSI is included. Frequency-domain response is also overestimated by both 1-D and 3 × 1-D input modes, with a strong dependence on source depth.

It is interesting to note the counterintuitive effect that omitting the vertical component (1-D case) might actually increase the response in some places of the structure. Compare, for example, Figure 10 with Figure 13, the peak horizontal response in terms of both displacements and accelerations at the base of the foundation is in fact increased by removing the vertical component. Looking at the discrete Fourier spectrum for the horizontal response in this case shows that even lower frequency components are affected in this case.

Because of the symmetry of this example, response at places like the foundation bottom and top of containment building show a decoupling of vertical and horizontal components, as can be seen as a flat response in the response at these points seen in Figures 8, 9, and 10. This is not the general case and is why looking at a different location, like the north-west corner of the auxiliary building, helps in understanding how vertical and horizontal components might interact.

Also noteworthy is the fact that vertical components of structural response for 1-D and 3 × 1-D input seem to match the response due to a full 3-D wave better than the horizontal components. This phenomenon can be partially

explained by the anisotropy of effective shear-wave speed present in this example. At 2.5 Hz, the implied wavelength for the top layer is 200 m, but that layer is only 50 m deep. Conceptually, this means that a wave at this frequency traveling along the layer, horizontally, can develop this wavelength but a vertically propagating wave will have a longer effective wavelength because it will mobilize deeper layers with higher wave speeds. Therefore, it is expected that this is a frequency-dependent phenomenon and the results would change at higher frequencies.

In the cross sections shown in Figure 16, showing displaced shape (heavily exaggerated), it is notable how the response at the DRM boundary is nearly identical in all 3 cases shown (3-D, 1-D and 3 × 1-D), except in that the 1-D case does not include the vertical component by definition. Also noteworthy is the visible flexing of the foundation slab, a phenomenon that has been experimentally measured before,[8, 9] in this case concentrated in the slab section separating auxiliary from containment buildings.

6 CONCLUDING REMARKS

The goal of ESSI modeling is to explicitly account for all processes that contribute to the seismic response of a soil-structure system, from source fault rupture, through crustal wave propagation, to soil-structural response and, finally, components. The DRM, by Bielak et al,[20] is the definitive tool that enables this process. Before the DRM, assumptions like the vertically incident plane-wave approximation were necessary to arrive at an answer but introduced modeling uncertainties that could not be evaluated because they could not be separated from other sources of uncertainty.

This work presents a step towards evaluating the modeling uncertainty introduced by the plane-wave approximations in the seismic response of soil-structure systems. Equivalent 1-D and 3 × 1-D wave-field approximations were developed from 3-D wave fields, obtained through numerical simulation, and the response of a soil-structure system to each of these was evaluated. Differences between the modeling approaches are not just in magnitude of the peak response, but in overall time-history shape and frequency content. By comparing the response of the structure to 3-D wave fields with the response to point-wise equivalent plane-wave approximations of the same motions, the relevance of full 3-D modeling is established. This conclusion coincides and extends the assessment of the United States Nuclear Regulatory Commission via document NUREG/CR-3805 on characterization of ground motions,[50] which appraises the importance of incidence angle (equivalently termed apparent velocity) and presence of surface waves in deciding whether a more complex approach is needed for ground motion modeling.

Despite the fact that the results shown herein seem to imply that assuming 1-D or 3×1-D wave fields is conservative with respect to the full 3-D wave field, it is very important to note that this is not a generalizable conclusion. Indeed, the results are very sensitive to all model parameters: structure, site,

and input motions. Therefore, the level of conservatism or unconservatism can be assessed only on a case-by-case basis with a full 3-D analysis. The role of regional heterogeneity, basin effects, nonlinear site response, sloping site, or presence of topography, among other complicating factors, in this context, has yet to be quantified. Because of the factibility of modeling these and other effects within the DRM framework without incurring in additional assumptions, the authors argue that performing ESSI analysis, given the right conditions, is a more rational and complete approach.

A maximum resolved frequency of 10 Hz was achieved in this study, which is insufficient to properly characterize all important aspects of NPP response pertaining to safety of its contents, but is enough to provide evidence that assuming a 1-D or 3 × 1-D wave comes with significant changes in response amplitude, shape, and frequency content. Achieving higher frequencies is an important goal to completely assess hazard to NPPs due to nearby faults. Modeling for higher frequencies becomes a significantly harder task both computationally and from a modeling standpoint. First, computational cost grows cubicly with maximum frequency such that achieving, say 30 Hz, is possible for a small near-field model like the one in this article if a larger HPC cluster is available. Regional-scale models are out of the question at this moment for these kinds of frequencies, though simulation programs like SW4 are getting ready for the next generation of exascale machines[51] that will tackle this problem. Second, and very importantly, modeling higher frequencies requires an adequate frequency-dependent representation of both anelastic attenuation (inherent damping) and scattering effects. Future work will look at extended sources, high-frequency motions, and the role of nonlinearity, but the intent of this paper was to develop fundamental understanding of the mechanics and which can be built upon to include these and many other features.

Realistic seismic modeling of the input DRM motions requires that complex, extended faults with multiple subfault segments, most commonly represented by linear superposition of point sources, be used (a concrete example on how to setup such a scenario can be found in Isbiliroglu et al[29]). In this way, it is possible to model important extended fault effects such as time-varying frequency content, pulse directivity, and longer duration motions with more motion-reversal cycles. These effects become important when evaluating nonlinear effects, especially in the presence of hysteresis. It is shown here, though, that the response discrepancies between models excited by full 3-D seismic fields and plane-wave approximations of these arise from the very element used to construct extended sources: the point source. Since large sources are compositions of point sources, these 3-D effects will be present for extended sources too.

For concrete applications, it is important that the earthquake models used to derive DRM input motions should also be able to reproduce, within uncertainties, the most important aspects of the motions observed at the seismic networks within the modeling region. In addition, it important to note

that the greatest flexibility of the DRM framework applied herein, by virtue of its completely physical formulation, is that it can also be used to postulate and evaluate new scenarios, which are plausible in the seismic setting but have never been observed and recorded.

ACKNOWLEDGEMENTS

The work presented in this paper was partially supported by the Canadian Nuclear Safety Commission (CNSC) and the United States Department of Energy (US DOE). This support is gratefully acknowledged.

REFERENCES

1. Wong HL, Luco JE. Dynamic response of rectangular foundations to obliquely incident seismic waves. Earthquake Engineering and Structural Dynamics. 1978;6:3-16. 2. NEHRP Consultants Joint Venture. Soil-Structure Interaction for Building Structures. Technical Report, Gaithersburg, MD, National Institute of Standards and Technology; 2012. 3. Housner GW. Interaction of building and ground during an earthquake. Bull Seism Soc Am. 1956;44(4):179-186. 4. Scanlan RH. Seismic wave effects on soil-structure interaction. Earthquake Engineering and Structural Dynamics. 1976;4(4):207-388. 5. Lee VW, Trifunac MD, Feng CC. Effects of foundation size on Fourier spectrum amplitudes of earthquake accelerations recorded in buildings. Int J Soil Dyn Earthquake Eng. 1982;1(2):52-58. https://doi.org/10.1016/0261-7277(82)90013-4 6. Trifunac M, Hao T, Todorovska MI. Response of a 14-story reinforced concrete structure to nine earthquakes: 61 years of observation in the Hollywood Storage Building (report CE 01-02). Technical Report, Los Angeles, California, Department of Civil Engineering, University of Southern California; 2001. 7. Trifunac MD, Todorovska MI, Orbovic N. A note on the motion of a large area on ground surface during passage of synthetic strong motion ´ waves. Soil Dyn Earthquake Eng. 2015;79:59-65. https://doi.org/10.1016/j.soildyn.2015.09.003 8. Trifunac MD, Ivanovc SS, Todorovska MI, Novikova EI, Gladkov AA. Experimental evidence for flexibility of a building foundation ´ supported by concrete friction piles. Soil Dyn Earthquake Eng. 1999;18(3):169-187. https://doi.org/10.1016/S0267-7261(98)00046-3 9. Ivanovic SS, Trifunac MD, Novikova EI, Gladkov AA, Todorovska MI. Ambient vibration tests of a seven-story reinforced concrete building ´ in Van Nuys, California, damaged by the 1994 northridge earthquake. Soil Dyn Earthquake Eng. 2000;19(6):391-411. https://doi.org/10. 1016/S0267-7261(00)00025-7 10. Luco JE. Torsional response of structures to obliquely incident seismic SH waves. Earthquake Eng Struct Dyn. 1976;4:207-219. 11. Luco JE, Wong HL. Response of structures to nonvertically incident seismic waves. Bull Seismol Soc Am. 1982;72(1):275-302. 12. Gicev V, Orbovic N, Trifunac MD. Two-dimensional translation, rocking, and waves in a building during soil-structure interaction excited ˇ by a plane SV-wave pulse. Soil Dyan Earthquake Eng. 2016;88:76-91. https://doi.org/10.1016/j.soildyn.2016.05.008 13. Gicev V, Trifunac MD,

Orbovi ˇ c N. Two-dimensional translation, rocking, and waves in a building during soil-structure interaction excited ´ by a plane earthquake P-wave pulse. Soil Dynamics and Earthquake Engineering. 2016;90:454-466. https://doi.org/10.1016/j.soildyn.2016. 01.006 14. Cao Y, Mavroeidis GP, Meza-fajardo KC, Papageorgiou AS. Accidental eccentricity in symmetric buildings due to wave passage effects arising from near-fault pulse-like ground motions. Earthquake Engineering & Structural Dynamic. 2017;46:2185-2207. https://doi.org/10. 1002/eqe 15. Jalali RS, Trifunac MD. A note on the wave-passage effects in out-of-plane response of long structures to strong earthquake pulses. Soil Dynamics and Earthquake Engineering. 2011;31:640-647. https://doi.org/10.1016/j.soildyn.2010.11.010 16. Wong HL, Trifunac MD. Interaction of a shear wall with the soil for incident plane SH waves: elliptical rigid foundation. Bull Seism Soc Am. 1974;64(6):1825-1842. 17. Luco JE, Sotiropoulos DA. Local characterization of free-field ground motion and effects of wave passage. Bull Seismol Soc Am. 1980;70(6):2229-2244. 18. Sykes LR, Armbruster JG, Kim W, Seeber L. Observations and tectonic setting of historic and instrumentally located earthquakes in the Greater New York City – Philadelphia Area. Bull Seismol Soc Am. 2008;98(4):1696-1719. 19. Hardebeck JL. Seismotectonics and fault structure of the California Central Coast. Bulletin of the Seismological of America. 2010;100(3):1031-1050. https://doi.org/10.1785/0120090307 20. Bielak J, Loukakis K, Hisada Y, Yoshimura C. Domain reduction method for three-dimensional earthquake modeling in localized regions. Part {I}: theory. Bull Seismol Soc Am. 2003;93(2):817-824. 21. Yoshimura C, Bielak J, Hisada Y. Domain reduction method for three-dimensional earthquake modeling in localized regions. Part {II}: Verif\/ication and Examples. Bull Seismol Soc Am. 2003;93(2):825-840. 22. Psarropoulos PN, Tazoh T, Gazetas G, Apostolou M. Linear and nonlinear valley amplification effects of seismic ground motion. Soils and Foundations, Japanese Geotechnical Society. 2007;47(5):857-871. 23. Jeremic B, Jie G, Preisig M, Tafazzoli N. Time domain simulation of soil-foundation-structure interaction in non-uniform soils. ´ Earthquake Eng Struct Dyn. 2009;38(5):699-718. https://doi.org/10.1002/eqe.896 24. Kontoe S, Zdravkovic L, Menkiti CO, Potts DM. Seismic response and interaction of complex soil retaining systems. Comput Geotech. 2012;39:17-26. https://doi.org/10.1016/j.compgeo.2011.08.003 25. Tripe R., Kontoe S., Wong T. KC. Slope topography effects on ground motion in the presence of deep soil layers. Soil Dyn Earthquake Eng. 2013;50:72-84. https://doi.org/10.1016/j.soildyn.2013.02.011 26. Jeremic B, Tafazzoli N, Ancheta T, Orbovi ´ c N, Blahoianu A. Seismic behavior of NPP structures subjected to realistic 3D, inclined seismic ´ motions, in variable layered soil/rock, on surface or embedded foundations. Nucl Eng Des. 2013;265:85-94. 27. Zhong R, Huang M. Winkler model for dynamic response of composite caisson-piles foundations: seismic response. Soil Dyn Earthquake Eng. 2014;66:241-251. http://linkinghub.elsevier.com/retrieve/pii/S0267726114001638. 28. Solberg JM, Hossain Q, Mseis G. Nonlinear time-domain soil-structure interaction

analysis of embedded reactor structures subjected to earthquake loads. Nucl Eng Des. 2016;304:100-124. http://linkinghub.elsevier.com/retrieve/pii/S0029549316300541. 29. Isbiliroglu Y, Taborda R, Bielak J. Coupled soil-structure interaction effects of building clusters during earthquakes. Earthquake Spectra. 2015;31(1):463-500. 30. Kuhlemeyer RL, Lysmer J. Finite element method accuracy for wave propagation problems. J Soil Mech Found Div. 1973;99:421-427. 31. Kouroussis G, Verlinden O, Conti C. Finite-dynamic model for infinite media: corrected solution of viscous boundary efficiency. J Eng Mech. 2011;137(7):509-511. https://doi.org/10.1061/(ASCE)EM.1943-7889.0000250 32. Elgamal A, Yan L, Yang Z, Conte JP. Three-dimensional seismic response of Humboldt Bay bridge-foundation-ground system. ASCE J Struct Eng. 2008;134(7):1165-1176. 33. Ostadan F, Deng N, Gurbuz O, Malushte S. Seismic soil-structure interaction analysis including ground motion incoherency effects. In: 14th World Conference on Earthquake Engineering (14WCEE); 2008; Beijing, China. Paper number: 04-02-0025. 34. Coleman JL, Bolisetti C, Whittaker AS. Time-domain soil-structure interaction analysis of nuclear facilities. Nucl Eng Des. 2015;298:264-270. https://linkinghub.elsevier.com/retrieve/pii/S0029549315003805. 35. Jeremic B, Jie G, Cheng Z, et al. The Real ESSI Simulator System: University of California, Davis and Lawrence Berkeley National ´ Laboratory; 2017. 36. Idriss IM, Sun JI. SHAKE91: A Computer Program for Conducting Equivalent Linear Seismic Response Analyses of Horizontally Layered Soil Deposits; 1992. 37. Mejia LH, Dawson EM. Earthquake deconvolution for FLAC. In: Proceedings of the 4th International FLAC Symposium on Numerical Modeling in Geomechanics. 29-31 May 2006; Madrid, Spain. 1-9. (1969). 38. Sjögreen B, Petersson NA. A fourth order accurate finite difference scheme for the elastic wave equation in second order formulation. J Sci Comput. 2011;52(1):17-48. https://doi.org/10.1007/s10915-011-9531-1. 39. Brune JN. Tectonic stress and the spectra of seismic shear waves from earthquakes. J Geophys Res. 1970;75(26):4997-5009. https://doi.org/10.1029/JB075i026p04997 40. Brune JN. Correction. J Geophys Res. 1971;76(20):5002. https://doi.org/10.1029/JB076i020p05002 41. Abell JA. Earthquake-soil-structure interaction modeling of nuclear power plants for near-field events. Ph.D. Thesis: University of California, Davis; 2016. 42. Geuzaine C, Remacle J-F. {Gmsh}: A {3-D} finite element mesh generator with built-in pre- and post-processing facilities. Int J Numer Methods Eng. 2009;79(11):1309-1331. https://doi.org/10.1002/nme.2579 43. Lysmer J, Kuhlemeyer RL. Finite dynamic model for infinite media. ASCE J Eng Mech Div. 1969;95(EM4):859-877. 44. Watanabe K, Pisanò F, Jeremic B. Discretization effects in the finite element simulation of seismic waves in elastic and elastic-plastic ´ media. Eng Comput. 2017;33(3):519-545. https://doi.org/10.1007/s00366-016-0488-4. 45. Courant R, Friedrichs K, Lewy H. On the partial difference equations of mathematical physics. Technical Report, New York, NY, U.S.A., Courant Institute of Mathematical Sciences, New York University; 1956. https://www.archive.org/details/onpartialdiffere00cour. 46.

Bergan PG, Felippa CA. A triangular membrane element with rotational degrees of freedom. Comput Meth Appl Mech Eng. 1985;50:25-69. 47. Alvin K, de la Fuente HM, Haugen B, Felippa CA. Membrane triangles with corner drilling freedoms – {I}. The {EFF} element. Finite Elem Anal Des. 1992;12:163-187. 48. Felippa CA, Militello C. Membrane triangles with corner drilling freedoms – {II}. The {ANDES} element. Finite Elem Anal Des. 1992;12:189-201. 49. Felippa CA, Alexander S. Membrane triangles with corner drilling freedoms – {III}. Implementation and Performance Evaluation. Finite Elem Anal Des. 1992;12:203-239. 50. Power MS, Chang CY, Idriss IM, Consultants WC, Kennedy RP, Inc SMA. US NRC Document NUREG/CR-3805, Vol. 5. Engineering Characterization of Ground Motion Task II : Summary Report, Walnut Creek, CA; 1986. 51. Johansen H, Rodgers AJ, Petersson NA, McCallen DB, Sjogreen B, Miah M. Toward exascale earthquake ground motion simulations for near-fault engineering analysis. Computing in Science and Engineering.2017;19(5):27-37.